

## REFERENCES

- [1] S. C. Cripps *et al.*, "An experimental evaluation of *X*-band mixers using dual-gate GaAs MESFET's," in *Proc. 7th European Microwave Conf.*, (Copenhagen), 1977, pp. 101-104.
- [2] C. Tsirones, R. Meirer, and R. Stahlmann, "Dual gate MESFET mixers," *IEEE Trans. Microwave Theory Tech.*, vol. MTT-32, pp. 248-255, Mar. 1984.
- [3] C. Tsirones *et al.*, "A self oscillating dual-gate GaAs MESFET *X*-band mixer with 12 dB conversion-gain," in *Proc. 9th European Microwave Conf.*, (Brighton, England), 1979, pp. 321-325.
- [4] O. S. A. Tang and C. S. Aitchison, "A very wide-band microwave MESFET mixer using the distributed mixing principle," *IEEE Trans. Microwave Theory Tech.*, vol. MTT-33, pp. 1470-1478, Dec. 1985.
- [5] A. Khanna, "Parallel feedback FETDRO design using 3-port S parameters," in *1984 IEEE MTT-S Dig.*, pp. 181-183.
- [6] A. Podcameni and L. Conrado, "Design of microwave oscillators and filters using transmission-mode dielectric resonators coupled to microstrip lines," *IEEE Trans. Microwave Theory Tech.*, vol. MTT-33, pp. 1329-1331, Dec. 1985.
- [7] H. Abe *et al.*, "A highly stabilized low-noise GaAs FET integrated oscillator with a dielectric resonator in *C* band," *IEEE Trans. Microwave Theory Tech.*, vol. MTT-26, pp. 156-162, Mar. 1978.
- [8] O. Ishihara *et al.*, "A highly stabilized GaAs FET oscillator using a dielectric resonator feedback circuit in 9-14 GHz," *IEEE Trans. Microwave Theory Tech.*, vol. MTT-28, pp. 817-824, Aug. 1980.
- [9] A. Khanna and Y. Garautt, "Determination of loaded, unloaded and external quality factors of a dielectric resonator coupled to a microstrip line," *IEEE Trans. Microwave Theory Tech.*, vol. MTT-31, pp. 261-264, Mar. 1983.
- [10] J. Altman, *Microwave Circuits*. New York: Van Nostrand, Reinhold, 1964.
- [11] C. P. Snapp, J. F. Kukielka, and N. K. Osbrink, "Practical silicon MMIC's challenge hybrids," *Microwaves and RF*, Nov. 1982.
- [12] J. Kukielka and C. Snapp, "Wideband monolithic cascadable feedback amplifiers using silicon bipolar technology," presented at 1982 IEEE Microwave and Millimeter-Wave Monolithic Circuits Symp., Dallas, TX.
- [13] G. C. Temes and S. K. Mitra, *Modern Filter Theory and Design*. New York: Wiley, 1973, pp. 49-53, 89-98.

## Dosimetry of Occupational Exposure to RF Radiation: Measurements and Methods

SANTI TOFANI AND GIOVANNI AGNESOD

**Abstract** — Workers engaged in the operation of RF industrial devices are exposed to electromagnetic radiation in the near-field zone that is characterized by high spatial and temporal gradients. The present paper is concerned with measurement methods and data analyses which allow the evaluation of the electromagnetic field exposure of the operator together with the SAR induced by near-field exposure accounting for the spatial and temporal variations. These methods are applied to the theoretical dosimetry of the occupational exposure to RF radiation emitted by 27.12-MHz plastic sealers. The data obtained are compared with those deducible through a conventional wide-band isotropic field meter.

### I. INTRODUCTION

The main features of the conditions of occupational exposure to electromagnetic fields that have to be considered for a correct dosimetry can be stated as follows:

- a) temporal nonuniformity of the emission from these devices;
- b) exposure of the operator standing near the device in near-field conditions with consequent nonuniform exposure to

Manuscript received September 14, 1986; revised February 3, 1987

The authors are with the Public Health Laboratory, National Health Service, Regione Piemonte USL 40, 10015 Ivrea, Italy.  
IEEE Log Number 8714113

the *E* and *H* fields with reference to the different body parts and lack of proportionality between the electric and magnetic components of the field;

- c) operator's mobility near the device because of the lack of a strictly fixed work position.

All these factors affect the mass-normalized power absorption rate (SAR) from the operator's body. The SAR is the parameter on the basis of which the threshold limits of the electromagnetic field exposure contained in guidelines [1] and [2] were defined in terms of external *E* and *H* fields [3], [4].

In recent years, many authors, among them Cox *et al.* [5], Conover *et al.* [6], Hietanen *et al.* [7], Stuchly *et al.* [8], and Gandhi *et al.* [9], have dealt with the evaluation of the exposure of workers charged with the operation of industrial devices to electromagnetic fields.

At present, a personal dosimeter capable of a direct measurement of the operator's SAR is not commercially available, although research on this kind of device is in progress [10], [11].

In such a situation, an accurate measurement of the electric and magnetic fields becomes of great importance. Indeed, through a knowledge of the behavior of these parameters, the operator's SAR can be estimated [12].

The theoretical prediction of SAR from only *E* field data is an acceptable approximation [12] when *E* fields predominate over *H* fields.

In the present paper, a measurement instrument which allows continuous monitoring of the electric field strength is shown. Further data analysis for an accurate estimation of the SAR of workers exposed to the near field of time-variable emission sources is presented.

Plastic sealers that are operated at a frequency of 27.12 MHz represent one of the more widespread sources of exposure to intense electromagnetic fields in occupational environments. These are the kind of devices we deal with.

For these devices, the leakage *E* field is the main electromagnetic factor related to the potential hazard.

The measurement instrument in this case has been used to estimate the component of the electric field only.

### II. INSTRUMENTS AND METHODS

For the continuous monitoring of the electric field strength to which the operator is exposed, we used an isotropic ( $\pm 1$  dB) wide-band electric-field probe connected to a battery-powered readout meter calibrated in a TEM cell at a frequency of 27.12 MHz with an accuracy of 0.7 dB [13] and supplying the rms value of the electric field. Such a meter is linked, by an optical fiber 10 meters long, to a repeater connected to the ac power main. The analog output of the repeater is connected to a graphic battery-operated recorder that is supplied. The graphic recorder and the repeater are contained in a shielded box equipped with a low-pass filter connected to the ac power main in order to suppress radiated or conducted RF due to the environmental 27.12-MHz electromagnetic field. The scheme of the instrumental chain is shown in Fig. 1. Measurements were carried out in a firm producing plastic accessories for cars.

The number of plastic sealers present in the firm is 14. The five devices with an output power of 6 kW and the six with an output power of 7.5 kW are not shielded and need to be manually loaded. The three remaining devices, with an output power of 25 kW, are shielded and automatically operated.

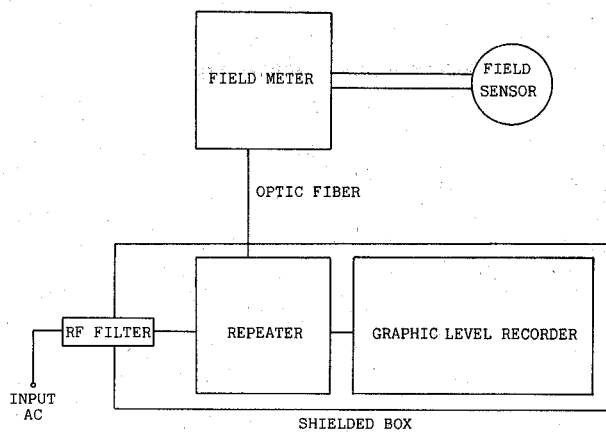
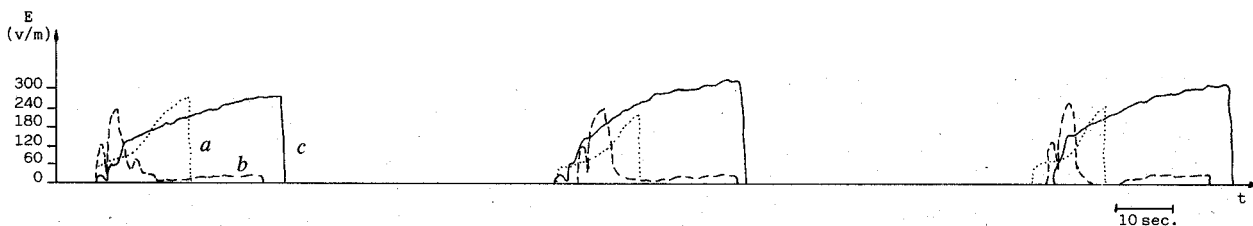


Fig. 1. Block diagram of the measurement instrumental chain.

Fig. 2. Plots of the electric field levels at three different operating conditions. Measurement height: 150 cm. Curve a (6-kW sealer):  $T = 1 \text{ min } 24 \text{ s}$ ,  $t = 15 \text{ s}$ . Curve b (6-kW sealer):  $T = 1 \text{ min } 24 \text{ s}$ ,  $t = 29 \text{ s}$ . Curve c (7.5-kW sealer):  $T = 1 \text{ min } 25 \text{ s}$ ,  $t = 32 \text{ s}$ .

Measurements were carried out to determine the temporal variation of the field strength at those fixed positions that are usually occupied by the operator. Measurements were carried out in the absence of the operator in order to avoid coupling between the same and the sensor. The data represent the temporal variation of the exposure during a current sealing process. Measurements were also carried out to determine the spatial variation of the field strength on a vertical axis in the absence of the operator and at fixed points to estimate the SAR of an operator immersed in such a field.

### III. RESULTS

The field strength levels change according to the device and the piece in work. Some examples of plots obtained by the instrumental chain described above are reported in Fig. 2. These plots are obtained at different operating conditions in the absence of the operator but at the position usually occupied by the same.

On the basis of these plots, it is possible, by means of time-dependent sampling, to compute the value of the rms exposure level  $E_{ON}$  for an operating device:

$$E_{ON} = \sqrt{\frac{\sum_i E_i^2}{N}} \quad (1)$$

A knowledge of  $E_{ON}$  makes it possible to accurately determine the mean value of the electric field  $E_A$  to which the operator is exposed during the whole working process, also taking into account the duty cycle (the ratio of working time  $t$  to the time  $T$  elapsing between two subsequent operations) according to the equation

$$E_A = E_{ON} \sqrt{\frac{t}{T}} \quad (2)$$

TABLE I  
MEAN VALUES OF THE ELECTRIC FIELD ( $E_{ON}$ ) DURING THE WORKING STAGE CORRECTED FOR THE DUTY CYCLE ( $E_A$ ) AND MAXIMUM VALUES ( $E_{MAX}$ ) OF THE ELECTRIC FIELD MEASURED FOR THE PROCESSES REPORTED IN FIG. 2

Plot	$E_{ON}$ (v/m)	$E_A$ (v/m)	$E_{MAX}$ (v/m)
a .....	141	60	220
b -----	69	41	215
c _____	203	125	265

Due to the unevenness of the field level, inferable from the plots of Fig. 2, it is very difficult to evaluate  $E_{ON}$  only by means of a wide-band isotropic field meter, such a meter allowing, at the best, a reading of the maximum and minimum levels of exposure. In Table I, for each plot the corresponding values of  $E_{ON}$ ,  $E_A$ , and the maximum value reached during the working stage  $E_{MAX}$  are reported.

From data reported in Table I, a great difference between the mean values  $E_{ON}$  and the maximum values  $E_{MAX}$  results. Moreover, the ratios of the two above-mentioned values can vary greatly for the same device according to the plastic piece being processed by the sealer (plots a and b of Fig. 2).

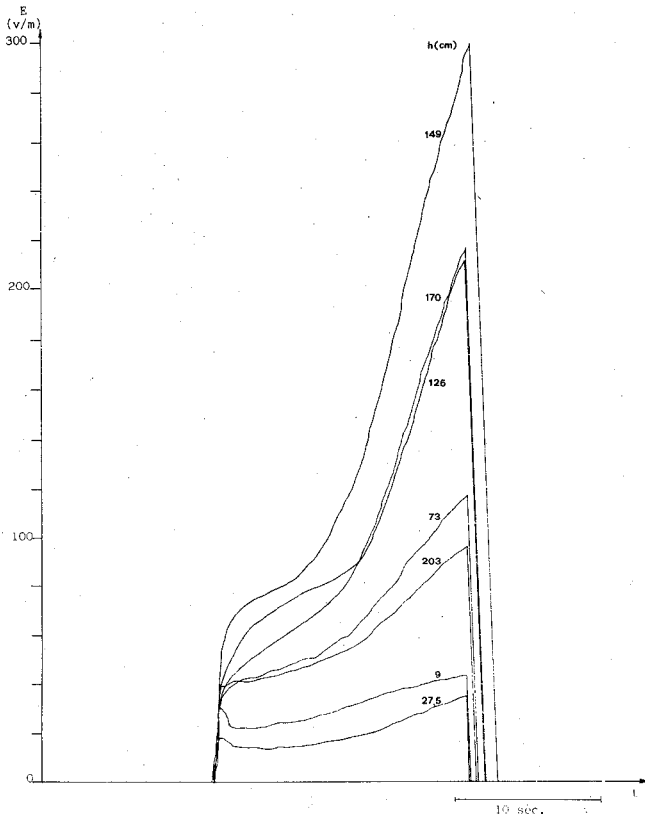


Fig. 3. Plots of the electric field levels at different heights above the floor, along the vertical axis corresponding to the operator position, during the processing of a series of equal plastic pieces. Number beside each plot indicates the height (in cm) at which measurement was carried out.

There is a more stringent need for a continuous recording of the exposure levels when the field variation depends both on the duty cycle and the operator's mobility.

As anticipated in the introduction, due to the exposure under near-field conditions, the operator is not immersed in a spatially uniform field. The electric field levels vary at a given moment along the vertical and horizontal axes depending on the operator's position. Besides the temporal mean, a determination of the spatial mean of the electric field level is needed.

In order to evaluate the influence of this spatial variation on the total exposure of the operator, the data of a plastic sealer with an output power of 6 kW are analyzed. The piece in work is the same as that of Fig. 2(a). Plots of the electric field strength at different heights of the operator position were taken during the working process. These plots are given in Fig. 3.

The mean value of the electric field strength  $E_{ON}$  has been calculated for each plot. In Fig. 4, data corresponding to the  $E_{ON}$  values, together with the  $E_{MAX}$  values obtained from the plots of Fig. 3, are reported.

The maximum field levels of  $E_{ON}$  and  $E_{MAX}$  are obtained at a height corresponding to the electrode height.

The SAR<sub>near-field</sub> can be estimated from the vertical profile of the electric field strength by means of the empirical equation proposed by Chatterjee *et al.* [14]. Such an equation allows one to calculate the approximate value of the average whole-body SAR<sub>near-field</sub> from the theoretically predicted value of the SAR<sub>far-field</sub> evaluated assuming conditions of exposure to an electric field having a uniform strength corresponding to the maximum value measured at the operator position.

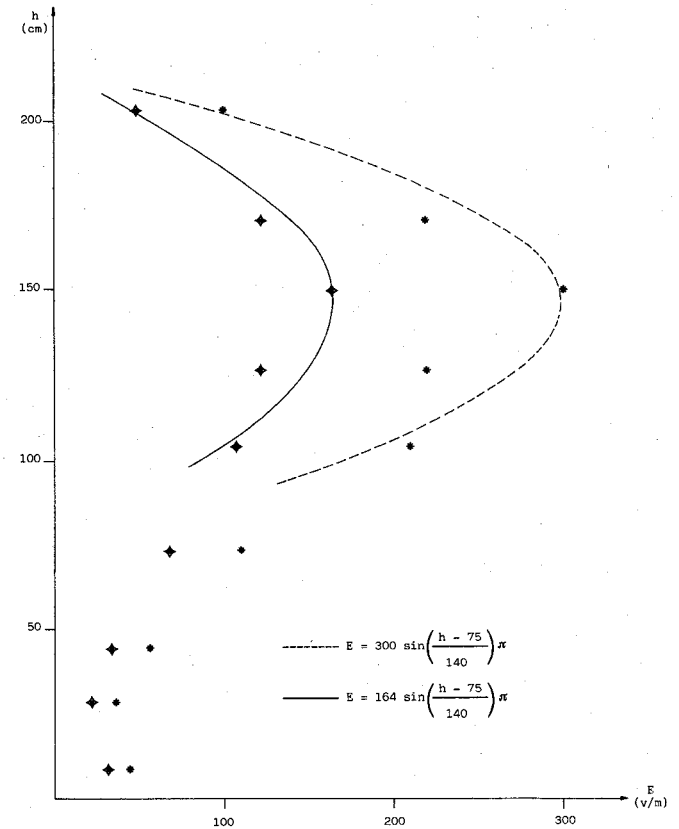


Fig. 4. Variation of the electric field levels along the vertical axis, corresponding to the position of the worker charged with the operation of the 6-kW plastic sealer, during the processing of the pieces of Fig. 3. Two sets of experimental points, corresponding, respectively, to the mean values  $E_{ON}$  and the maximum value  $E_{MAX}$ , are reported.

Disregarding the horizontal variation of the electric field along the operator's width, the above-mentioned equation becomes

$$\text{SAR}_{\text{near-field}} = \frac{\text{SAR}_{\text{far-field}}}{1 + \frac{(A_V)^2}{(\Delta_V)^2}} \quad (3)$$

where the parameter  $A_V$  (depending on both the frequency and the electric-field polarization) is tabulated in the above-mentioned work, while the parameter  $\Delta_V$  is deducible from the vertical profile of Fig. 4. The analytical form of these functions, obtained by fitting the experimental data, is also reported in Fig. 4. Because of the ground reflection, the measurements obtained at a height less than 75 cm are not considered in the interpolation. The maximum value of the function is located at a height equal to that of the sealer's applicators. The SAR<sub>far-field</sub> value can be inferred from a table in the *Radiofrequency Radiation Dosimetry Handbook* [15].

The SAR<sub>near-field</sub> obtained from the  $E_{ON}$  and  $E_{MAX}$  values in Fig. 4 by means of (3), are  $1.2 \times 10^{-1}$  W/kg and  $4.2 \times 10^{-1}$  W/kg, respectively.

The ratio of these values, equal to 3.5, remains unchanged when applying both correction factors for a duty cycle equal to 0.42.

#### IV. CONCLUSIONS

Results reported in the present work illustrate the fact that, for a correct evaluation of the exposure to RF electromagnetic fields originating from industrial dielectric sealers, continuous monitor-

ing of the rms electric and magnetic field values together with a graphic or magnetic recording is essential.

Using the above-described methods, the spatial and temporal mean of the electric field rather than the mean of the maximum values can be determined. The maximum values, obtained on the integration time of the probe, are nearly the only ones obtainable using the customary wide-band isotropic field meters.

By means of the electric field values thus obtained, the actual whole-body-averaged power absorption rate (SAR) can be estimated.

From the above-reported example, it is seen that noncontinuous monitoring of the field levels would lead to an overestimation of the electric field and of the SAR. We have shown that the SAR overestimation, equal to the ratio of the two different values of the SAR<sub>near-field</sub>, obtained from the values of  $E_{ON}$  and  $E_{MAX}$ , respectively, can reach a value of 3.5.

On the basis of this work, it seems that technical recommendations or guidelines should consider the measurement instrument characteristics and the methods that must be used to determine compliance with the exposure thresholds contained in the RF radiation safety regulations.

#### REFERENCES

- [1] *Threshold Limit Values for Physical Agents in the Work Environment Adopted by ACGIH with Intended Changes for 1985-86*, American Conference of Government Industrial Hygienists.
- [2] *Safety Levels with Respect to Human Exposure to Radiofrequency Electromagnetic Fields, 300 kHz to 100 GHz*, ANSI Committee C95.1, 1982.
- [3] Food and Drug Administration, "Guidance for radio frequency sealers and dielectric heaters," in *Proc. 17th Ann. Nat. Conf. Radiation Control*, Dec. 1985, pp. 336-341.
- [4] *Dielectric (RF) Heater Guidelines for Limiting Radiofrequency Exposure*, Health and Welfare Canada Document 80-EHD-58, 1980.
- [5] C. Cox, W. E. Murray, Jr., and E. D. Foley, Jr., "Occupational exposures to radiofrequency radiation (18-31 MHz) from RF dielectric heat sealers," *Amer. Ind. Hyg. Ass. J.*, vol. 43, pp. 149-153, Mar. 1982.
- [6] D. L. Conover, W. E. Murray, Jr., E. D. Foley, J. M. Lary, and W. H. Parr, "Measurement of electric- and magnetic-field strengths from industrial radio-frequency (6-38 MHz) plastic sealers," *Proc. IEEE*, vol. 68, pp. 17-20, Jan. 1980.
- [7] M. Hietanen, K. Kalliomäki, P. L. Kalliomäki, and P. Linfords, "Measurement of strengths of electric and magnetic fields near industrial radio-frequency heaters," *Radio Sci.*, vol. 14 pp. 31-33, Nov./Dec. 1979.
- [8] M. A. Stuchly and D. W. Lecuyer, "Induction heating and operator exposure to electromagnetic fields," *Health Phys.*, vol. 49, pp. 693-700, Nov. 1985.
- [9] O. P. Gandhi, J. Y. Chen, and A. Riazi, "Currents induced in a human being for a plane-wave exposure conditions 0-50 MHz and for RF sealers," *IEEE Trans. Biomed. Eng.*, vol. BME-33, pp. 757-767, Aug. 1986.
- [10] O. P. Gandhi, I. Chatterjee, D. Wu, and Y. G. Gu, "Likelihood of high rates of energy deposition in the human legs at the ANSI recommended 3-30 MHz RF safety levels," *Proc. IEEE*, vol. 73, pp. 1145-1147, June 1985.
- [11] R. A. Tell, "Real-time data averaging for determining human RF exposure," presented at the 1986 Convention, National Association of Broadcasters, Washington, DC.
- [12] I. Chatterjee, M. J. Hagmann, and O. P. Gandhi, "Electromagnetic energy deposition in an inhomogeneous block model of man for near-field irradiation conditions," *IEEE Trans. Microwave Theory Tech.*, vol. MTT-28, pp. 1452-1459, Dec. 1980.
- [13] S. Tofani, L. Anglesio, G. Agnesod, and P. Ossola, "Electromagnetic standard fields: Generation and accuracy levels from 100 kHz to 990 MHz," *IEEE Trans. Microwave Theory Tech.*, vol. MTT-34, pp. 832-835, July 1986.
- [14] I. Chatterjee, O. P. Gandhi, and M. J. Hagmann, "Numerical and experimental results for near-field electromagnetic absorption in man," *IEEE Trans. Microwave Theory Tech.*, vol. MTT-30, pp. 2000-2005, Nov. 1982.
- [15] C. H. Durney, C. C. Johnson, P. W. Barber, H. Massoudi, M. F. Iskander, J. L. Lords, D. K. Ryser, J. S. Allen, and J. C. Mitchell, *Radiofrequency Radiation Dosimetry Handbook*, 2nd ed. (edited by USAF School of Aerospace Medical Division, Brooks Air Force Base, TX), 1978.

#### Decade Bandwidth Bias T's for MIC Applications up to 50 GHz

B. J. MINNIS

**Abstract** — A new design of bias T is described capable of carrying direct currents (dc) of a number of amperes while operating over RF bandwidths of more than a decade. Realized in microstrip or stripline, a design can operate up to at least 50 GHz as either a stand-alone component or as part of a microwave integrated circuit (MIC). The bias T circuit has been treated as a combination of HP, BP, and LP filters, the BP filter forming the major part. Design of the filter is by an exact transfer function synthesis procedure involving the application of the Richards transformation [1].

#### I. INTRODUCTION

Bias T's are used for feeding dc power to active RF components in such a way that the RF behavior of the component is not adversely affected by the dc connection. They behave as diplexers which in the ideal case comprise a pair of LP and HP filters with a cutoff frequency just above zero (dc). Large current capacities and broad bandwidth capabilities have, in the past, been difficult to achieve without using elaborate, expensive methods of construction. However, the design described in this paper is capable of handling dc in excess of 3 A, and RF bandwidths of over a decade are possible with operating frequencies reaching as high as 50 GHz. It is suitable for realization in microstrip or triplate stripline and can be constructed as a low-cost individual component or, alternatively, made to form part of a more complex microwave integrated circuit (MIC).

This paper will describe the basic structure of the bias T, its equivalent circuit, and the synthesis procedure used in its design. Two practical examples will be given which cover the bands 1.8-18.2 GHz and 4.5-45.5 GHz, respectively.

#### II. BASIC BIAS T AND EQUIVALENT CIRCUIT

The concept of a bias T as a diplexer comprising LP and HP filters is illustrated in Fig. 1(a). It has been common practice for designers of bias T's to concentrate on only the LP element in this combination. Often, the HP element comprises only a series capacitor, while the LP element is a more complicated arrangement of transmission lines, stubs, capacitors, and in some cases resistors. A simple example in widespread use is that illustrated in Fig. 1(b). The LP filter is a transmission line terminated in a shunt capacitor, and the maximum realizable impedance of the line limits the frequency bandwidth. Bandwidths of 3:1 are the typical limit for this bias T.

The aim with the new design was to produce a bias T with decade bandwidth performance at microwave frequencies suitable for printed-circuit realization. This has been achieved by giving attention to the design of the diplexer as a whole, instead of concentrating on the LP filter. Conceptual changes to the filter combination are indicated in the functional diagram of Fig. 2. Most significantly, a BP filter has been added, which, although shown as a pair of filters in the diagram, is a single filter with a

Manuscript received August 2, 1986; revised December 19, 1986.

The author is with the Systems Division of Philips Research Laboratories, Redhill, Surrey RH1 5HA England.

IEEE Log Number 8714117.